NASA MEMO 11-30-58A

NASA

MEMORANDUM

EXPERIMENTAL WIND-TUNNEL INVESTIGATION OF THE

TRANSONIC DAMPING-IN-PITCH CHARACTERISTICS

OF TWO WING-BODY COMBINATIONS

By Horace F. Emerson and Robert C. Robinson

Ames Research Center
Moffett Field, Calif.

NATIONAL AERONAUTICS AND SPACE ADMINISTRATION

WASHINGTON

December 1958

NATIONAL AERONAUTICS AND SPACE ADMINISTRATION

MEMORANDUM 11-30-58A

EXPERIMENTAL WIND-TUNNEL INVESTIGATION OF THE TRANSONIC DAMPING-IN-PITCH CHARACTERISTICS OF TWO WING-BODY COMBINATIONS

By Horace F. Emerson and Robert C. Robinson

SUMMARY

The results of an experimental wind-tunnel investigation of the damping in pitch of two wing-body combinations are presented. The tests were conducted in the Ames 14-foot transonic wind tunnel over a Mach number range from 0.60 to 1.18. Reynolds numbers varied from 2.3 million to 5.5 million. One model with a triangular wing of aspect ratio 2 having NACA 0003-63 sections was oscillated at an amplitude of 1.5° and a frequency of 17 cycles per second. The second model with a straight, tapered wing of aspect ratio 3 having 3-percent biconvex circular-arc sections was oscillated at an amplitude of 1.0° and a frequency of 21 cycles per second. The tests were made with the models at a mean angle of attack of 0°.

The models were oscillated with a dynamic balance that was actuated by an electrohydraulic servo valve. The results of this investigation indicate the usefulness of this new apparatus.

The experimental results of a previous damping-in-pitch investigation conducted in the Ames 6- by 6-foot supersonic wind tunnel at Mach numbers from 1.2 to 1.7 are included along with the theoretical results for this Mach number range. In the region of Mach numbers available for comparison, good agreement is shown to exist between the data obtained in the two facilities, except for some inconsistency in the slopes of the curves at $M = 1.2$ for the triangular wing.

The results of this investigation clearly show that for the models tested the maximum values of the damping in pitch occur at Mach numbers very close to 1.0, and that abrupt changes in the pitch damping are encountered near sonic velocity.

INTRODUCTION

With increased attention being focused on the dynamic characteristics of both piloted and pilotless flight vehicles, considerable interest has recently been evidenced in research equipment capable of providing accurate experimental information on the rotary derivatives.

At the Ames Aeronautical Laboratory, wind-tunnel data on the dynamic behavior of models have been obtained with free-oscillation equipment (see, e.g., refs. 1 and 2) and with forced-oscillation equipment (see, e.g., refs. 3, 4, and 5). The references cited covered a Mach number range from 0.23 to 1.9 with the exception of that part of the transonic Mach number range extending from 0.95 to 1.2.

Exclusion of this range was due to the well-known limitations of solid-wall wind tunnels at transonic speeds and was particularly unfortunate in the study of dynamic stability, since the trends of the data clearly showed that the most significant changes in the damping were likely to occur in that speed range. Later, of course, the introduction of the perforated test section extended the usefulness of the wind tunnel through the transonic speed range. To provide equipment suitable for wind-tunnel studies of dynamic stability in this range, a balance was designed and built for the Ames 14-foot wind tunnel. The present report includes a description of the electrohydraulic equipment employed and presents the results of experiments with two wing-body combinations which previous investigations had indicated would show markedly different behavior in the transonic range.

NOTATION

A aspect ratio, $\frac{b^2}{S}$

C_m pitching-moment coefficient, $\frac{\text{pitching moment}}{(1/2)\rho_\infty V_\infty^2 S\bar{c}}$

I moment of inertia, slug-ft^2

K restoring moment per unit angular deflection, ft-lb/radian

M_∞ free-stream Mach number, $\frac{V_\infty}{a_\infty}$

P damping moment per time rate of change of angle of attack, ft-lb-sec

R Reynolds number, based on wing mean aerodynamic chord

S wing area, including portion enclosed by body, sq ft

T_S tunnel stagnation temperature, $^\circ$F

V_∞ free-stream velocity, ft/sec

a_∞ speed of sound in free stream, ft/sec

b wing span, ft

c wing root chord, ft

$\bar{c}$ wing mean aerodynamic chord, $\frac{2}{S}\int_0^{b/2} c^2 dy$, ft

f frequency of oscillation, cps

k reduced frequency parameter, $\frac{\omega\bar{c}}{2V_\infty}$

t time, sec

q angular velocity due to pitching, radians/sec

q_∞ free-stream dynamic pressure, $\frac{1}{2}\rho_\infty V_\infty^2$, lb/sq ft

y spanwise coordinate, measured from line of symmetry of wing, ft

α angle of attack of wing chord plane, deg

$\dot{\alpha}$ time rate of change of angle of attack, radians/sec

α_o oscillation amplitude (one-half of peak-to-peak value), deg

ρ_∞ mass density of air, slugs/cu ft

ω angular frequency of oscillation, $(2\pi f)$, radians/sec

When α, $\dot{\alpha}$, and q are used as subscripts, a dimensionless derivative is indicated, and this derivative is evaluated as the independent variable (α, $\dot{\alpha}$, or q) approaches zero; for example,

$$C_{m_\alpha} = \left(\frac{\partial C_m}{\partial \alpha}\right)_{\alpha \to 0} \qquad C_{m_q} = \left[\frac{\partial C_m}{\partial (q\bar{c}/2V_\infty)}\right]_{q \to 0} \qquad C_{m_{\dot{\alpha}}} = \left[\frac{\partial C_m}{\partial (\dot{\alpha}\bar{c}/2V_\infty)}\right]_{\dot{\alpha} \to 0}$$

A dot above a symbol denotes a derivative with respect to time. Angles, forces, and moments are referred to the center of rotation of the wing and are positive as indicated in figure 1.

APPARATUS AND TESTS

Wind Tunnel

This investigation was conducted in the Ames 14-foot transonic wind tunnel. The 14-foot wind tunnel is a closed-circuit tunnel with convergent-divergent flexible walls and a perforated test section, and

operates at atmospheric total pressure. The wind tunnel is continuously operable from subsonic to low supersonic speeds. Figure 2 presents the general arrangement of the high-speed portion of the tunnel.

Models

Plan views of the two wing-body combinations are shown in figure 3. These are two of the models that were investigated in the Ames 6- by 6-foot wind tunnel and reported in reference 2, except that the laminated-wood forebodies and aluminum afterbodies were replaced with bodies fabricated of a Fiberglas and plastic laminate. The same body shapes, airfoil sections, and plan forms were retained. One configuration was an aspect-ratio-2 triangular wing having NACA 0003-63 sections in streamwise planes. The other was an aspect-ratio-3, straight, tapered wing having 3-percent symmetrical circular-arc sections. These two wing-body combinations were chosen to provide a broad range of variation of damping-in-pitch coefficient with Mach number, in both the stable and unstable regions.

Model Support System

The dynamic balance with its drive system was mounted on the regular sting and sting support of the 14-foot transonic wind tunnel. The models to be tested were mounted on the dynamic balance. Figure 4 presents a photograph of one of the models in the wind tunnel. The vertical strut shown in the photograph is attached to a 2000 pound weight through a variable viscous damper. The weight on the strut reduces the natural frequency of the model support system to 3 or 4 cycles per second, and the damper is used to reduce the amplitude of any support system oscillation that may occur. The cables shown in the photograph were very effective in preventing lateral vibration of the long, slender strut. At the model oscillation frequencies used in the present investigation, the sting response was negligible.

Figures 5(a) and 5(b) show an assembled view of the dynamic balance and the essential components of its drive system. An electrohydraulic servo valve ports oil alternately to either side of the drive piston. The motion is imparted to the model through a torque arm that is driven by a cable (fig. 5(a)). The cable is under tension at all times and does not transmit any appreciable torque due to position. An alternative method making use of a carefully fitted pin and solid connecting link at the top of the torque arm was also used (fig. 5(b)). This alternative method made it possible to dispense with the return spring. Both systems yielded results that were in close agreement. Figure 6 presents a photograph of the dynamic balance with the solid connecting link.

A block diagram of the electrohydraulic drive system is presented in figure 7. Further discussion of the hydraulic system may be found in the appendix.

Resistance-type wire strain gages were applied to the torque arm and to the cantilever springs to provide electrical signals proportional respectively to the total torque experienced by the model and to the model position.

The cantilever springs and crossed-flexure pivots provided the necessary spring-restoring moment to operate the system near resonance.

Tests

The wind-tunnel tests were conducted over a Mach number range from 0.60 to 1.18. Corresponding Reynolds numbers over the range of stagnation temperatures encountered are presented as functions of Mach number in figure 8. All of the wind-tunnel tests were made with the model at a mean angle of attack of 0°. The triangular wing was oscillated at an amplitude of 1.5° and a frequency of 17 cycles per second. The straight, tapered wing was oscillated at an amplitude of 1.0° and a frequency of 21 cycles per second.

The models tested, the range of their moments of inertia, minimum and maximum Reynolds numbers, the axes of rotation, and the ranges of reduced frequencies are given in the following table:

Model	Range of moment of inertia, slug-ft^2	Reynolds number, million	Axes of rotation, percent $\bar{c}$	Range of reduced frequency
A = 2 triangular	0.0766 - 0.0879	3.6 - 5.5	35, 45	0.050 - 0.095
A = 3 straight tapered	0.0506 - 0.0543	2.3 - 3.6	20, 35	0.041 - 0.078

Reduction of Data

The out-of-phase or damping moments with which this investigation is concerned were measured by means of equipment known as the NACA Ames flutter analyzer. A block diagram of the flutter analyzer is presented in figure 9. This readout equipment functions in the same manner as a wattmeter. The electrical analog of position is introduced into the equipment and shifted through a phase angle of 90°. The electrical analog of torque is also introduced and the product, which is read on the output meter, is directly proportional to the damping loads experienced by the

model. Before each wind-tunnel run the meter is adjusted to zero while the model is oscillating. This procedure takes account of any wind-off damping that may exist.

Because of the calibration procedure used with the readout equipment, it was not possible to change the frequency of the forced oscillation from the wind-off to the wind-on condition. As a result the wind-on natural frequency which is affected by the aerodynamic spring forces could not be determined. For this reason values of C_{m_α} were not obtained.

Corrections to Data

No corrections were applied to the data. Tunnel-wall-interference effects and tunnel air-stream inclination were considered to be negligible. Very little is known about the effect of tunnel resonance in transonic tunnels, but it is believed that the small models used in this investigation, in conjunction with the perforated walls, make such a correction unnecessary.

Precision of Data

A calibration of the accuracy of the flutter analyzer showed it to introduce an error in the damping component of 1.4 percent. A systematic error of this magnitude could easily be introduced by small phase shifts in the amplifiers or by failure of the phase shifter to rotate the position signal exactly 90°. Errors introduced in the wind-tunnel data due principally to harmonic content induced in the signal with a resultant deterioration of the wave form increased the probable error in the damping component to 5 percent at the higher Mach numbers.

The free-stream Mach number is accurate to within ±0.002; the mean angle of attack was determined with the wind off to an accuracy of $\pm 0.01^\circ$. The oscillation amplitude was determined visually and has an accuracy of $\pm 0.1^\circ$. The frequency of the oscillation amplitude was determined from the calibrated dial of a commercially available signal generator and is known to be accurate to within ±0.1 cycle per second over the range used.

RESULTS AND DISCUSSION

The experimental results of this investigation for the damping-in-pitch coefficient $C_{m_q} + C_{m_{\dot{\alpha}}}$ are shown plotted as a function of Mach number in figures 10 and 11. Also shown in figures 10 and 11 are the theoretical and experimental damping-in-pitch results from reference 2 for the two wing-body combinations of the investigation reported herein.

Aspect-Ratio-2 Triangular Wing

The data presented in figure 10(a) show that for the aspect-ratio-2 triangular wing oscillated about the 45-percent point of the mean aerodynamic chord the damping in pitch increased rapidly between Mach numbers of 0.60 and 0.98, reaching a maximum value of $C_{m_q} + C_{m_{\dot{\alpha}}}$ of -1.85. As the Mach number is further increased, the damping-in-pitch coefficient decreases rapidly but does not become unstable. Figure 10(b) presents data obtained with the triangular wing oscillating about the 35-percent point of the mean aerodynamic chord, and indicates that the model exhibits much the same variation of damping-in-pitch coefficient with Mach number. The maximum value of $C_{m_q} + C_{m_{\dot{\alpha}}}$ again occurs at a Mach number of 0.98 with the somewhat higher value of -2.40.

It can be seen in figure 10(b) that the data from this investigation agree extremely well with the subsonic results from reference 2. At supersonic Mach numbers, however, some differences exist between the results from the two facilities, the present results being higher than those of reference 2 for an axis at 0.45 $\bar{c}$ (fig. 10(a)) and lower for an axis at 0.35 $\bar{c}$ (fig. 10(b)). Although the differences are not large (on the order of 0.3) the inconsistencies in the slopes of the curves at $M = 1.2$ (figs. 10(a) and (b)) suggest that further data are required to establish more firmly the behavior of the damping coefficient in this range of Mach numbers.

Straight, Tapered Wing

Figure 11(a) shows the damping-in-pitch coefficient for the aspect-ratio-3, straight, tapered wing oscillating about the 35-percent point of the mean aerodynamic chord. Some noteworthy differences are apparent between the results for the two wing-body combinations. The maximum value of $C_{m_q} + C_{m_{\dot{\alpha}}}$ of -6.2 is considerably higher than the values obtained with the triangular wing and the peak value occurs at a Mach number of 0.95. The trend established with the triangular wing, of a rapid loss in stability from a peak value, was arrested at a Mach number of 0.98 and the data show that the value of $C_{m_q} + C_{m_{\dot{\alpha}}}$ remained essentially constant to a Mach number of 1.06 before resuming the trend toward neutral stability. Additional data points were taken to insure that the variation shown in figure 11(a) was not in error. Repeated points and points at additional Mach numbers served to confirm the variation of $C_{m_q} + C_{m_{\dot{\alpha}}}$ shown in figure 11(a). The difference between the data from this investigation and those of reference 2 at $M = 1.2$ in terms of the damping-in-pitch parameter is again about 0.3 for both wings.

Figure 11(b) presents the results obtained with the aspect-ratio-3, straight, tapered wing oscillating about the 20-percent point of the mean aerodynamic chord. The damping-in-pitch coefficient increases smoothly

with increasing Mach number to a maximum value of -8.8 at Mach number of 0.96. A very slight further increase in Mach number results in the configuration becoming unstable. The drive system could not control the model in an unstable condition and hence no data were obtained above a Mach number of 0.98.

Over the Mach number range at which pitch damping was stable, two separate sets of data are plotted. The spring-cable drive system, shown in figure 5(a), was used to obtain one set of data while the fitted pin and connecting link system shown in figure 5(b) was used to obtain the other set. The trends of the data are identical.

CONCLUDING REMARKS

The data presented show the variation of the damping-in-pitch coefficient for an aspect-ratio-2 triangular wing and an aspect-ratio-3, straight, tapered wing through the range of Mach numbers from 0.60 to 1.18. These first tests established the usefulness of the apparatus over the Mach number range where stable values of $C_{m_q} + C_{m_{\dot{\alpha}}}$ were encountered. The triangular wing was oscillated at an amplitude of 1.5° and a frequency of 17 cycles per second; the straight wing was oscillated at an amplitude of 1.0° and a frequency of 21 cycles per second. All tests were made with the models at a mean angle of attack of 0°. Within the test limitations the results of this investigation show that the maximum values of the damping in pitch occur at Mach numbers very close to 1.0, and that abrupt changes in pitch damping are encountered near sonic velocity.

Ames Research Center
National Aeronautics and Space Administration
Moffett Field, Calif., Sept. 16, 1958

APPENDIX

FURTHER NOTES ON THE ELECTROHYDRAULIC DRIVE SYSTEM

When the decision was made to measure rotary-stability derivatives in the 14-foot transonic wind tunnel, it was realized that a more powerful means of oscillating the models was required than the electromagnetic shakers which had been used successfully in variable-density wind tunnels (see ref. 5).

With the model oscillating at resonance, it is only necessary to introduce into the oscillatory system sufficient power to overcome the aerodynamic damping component. The determination of the power requirements for such a system, making use of the experimentally determined values of $C_{m_q} + C_{m_{\dot{\alpha}}}$ and the model dimensions from this investigation, is shown below

$$C_{m_q} + C_{m_{\dot{\alpha}}} = - \frac{4P_o}{\rho_\infty V_\infty S \bar{c}^2} \qquad \text{(see ref. 1)}$$

where P_o is the aerodynamic damping and has the dimensions lb-ft-sec. The expression to evaluate P_o may be rewritten

$$P_o = - \frac{(C_{m_q} + C_{m_{\dot{\alpha}}}) \rho_\infty V_\infty S \bar{c}^2}{4}$$

Using the following values for the straight, tapered wing of aspect ratio 3 in the above equation:

$C_{m_q} + C_{m_{\dot{\alpha}}}$	-8.8
S	1.54 ft^2
$\bar{c}$	0.76 ft
ρ_∞ (M = 0.96)	0.00156 slugs/cu ft
V_∞ (M = 0.96)	986 ft/sec

gives

$$P_o = 3 \text{ ft-lb-sec}$$

The example wing was oscillated at 21 cycles per second at an amplitude of 1.0^o. The torque required of the drive system is:

$$M = P_o\dot{\alpha} = \frac{(3)(2\pi)(21)(1.0)}{57.3} = 6.93 \text{ ft-lb} = 83.2 \text{ in-lb}$$

The maximum torque available from the electromagnetic shaker systems in use at this laboratory does not exceed 50 in-lb.

Of the various types of drive systems with the necessary power capability that were investigated, the electrohydraulic servo-valve system was selected. It held the promise of relative system simplicity, versatility of frequency and amplitude range, and high power capability.

The servo valve used was a Moog Valve Company Model 2000. This valve was operated at a line pressure of 3000 pounds per square inch which, when valve and line losses are accounted for, results in a pressure application to the piston of 2000 psi. The piston used had a net area of approximately 0.7 sq in. This results in a net force application of 1400 pounds if it is required. The torque arm used in the drive system was 1.75 inches long and thus the torque available at the model is 2450 in-lb.

Considerable difficulty has been encountered with the phase shift through the servo valve and through the torque arm. At the present time the system is seriously limited by these phase shifts. It is possible for the phase to shift 180° or more and render the drive system unstable. With this type of drive system in its present state of development, a drive system instability tends to drive the oscillator at a higher frequency than the resonant frequency determined from the cantilever springs and crossed flexure pivots. The unstable frequency is determined by the spring rate of the torque arm when it is added to the other springs in the system. Efforts are being made to increase the stiffness of the torque bar to the point where it will not interfere with the desired resonant frequency, and yet where it will still act as a satisfactory torque transducer.

The only serious disadvantage of the electrohydraulic servo-valve drive system is the one outlined above. Satisfactory results can be obtained in the negative (or stable) range of $C_{m_q} + C_{m_{\dot{\alpha}}}$ at the present time. It is felt that additional effort will see the usefulness of this device extended to provide reliable aerodynamic results through the unstable range of $C_{m_q} + C_{m_{\dot{\alpha}}}$.

REFERENCES

1. Tobak, Murray, Reese, David E., Jr., and Beam, Benjamin H.: Experimental Damping in Pitch of 45° Triangular Wings. NACA RM A50J26, 1950.

2. Tobak, Murray: Damping in Pitch of Low-Aspect-Ratio Wings at Subsonic and Supersonic Speeds. NACA RM A52L04a, 1953.

3. Beam, Benjamin H.: The Effects of Oscillation Amplitude and Frequency on the Experimental Damping in Pitch of a Triangular Wing Having An Aspect Ratio of 4. NACA RM A52G07, 1952.

4. Lessing, Henry C., Fryer, Thomas B., and Mead, Merrill H.: A System for Measuring the Dynamic Lateral Stability Derivatives in High-Speed Wind Tunnels. NACA TN 3348, 1954.

5. Beam, Benjamin H.: A Wind-Tunnel Test Technique for Measuring the Dynamic Rotary Stability Derivatives at Subsonic and Supersonic Speeds. NACA Rep. 1258, 1956. (Supersedes NACA TN 3347).

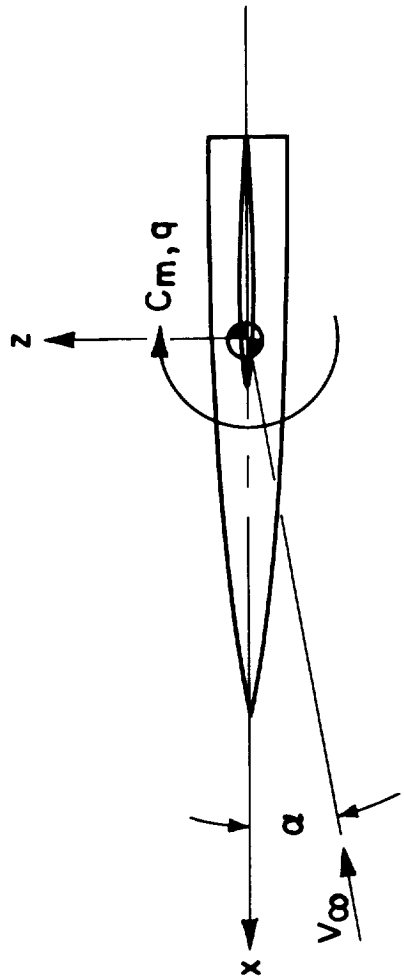

Figure 1.- Angles, forces, and moments shown in their positive directions about the center of rotation.

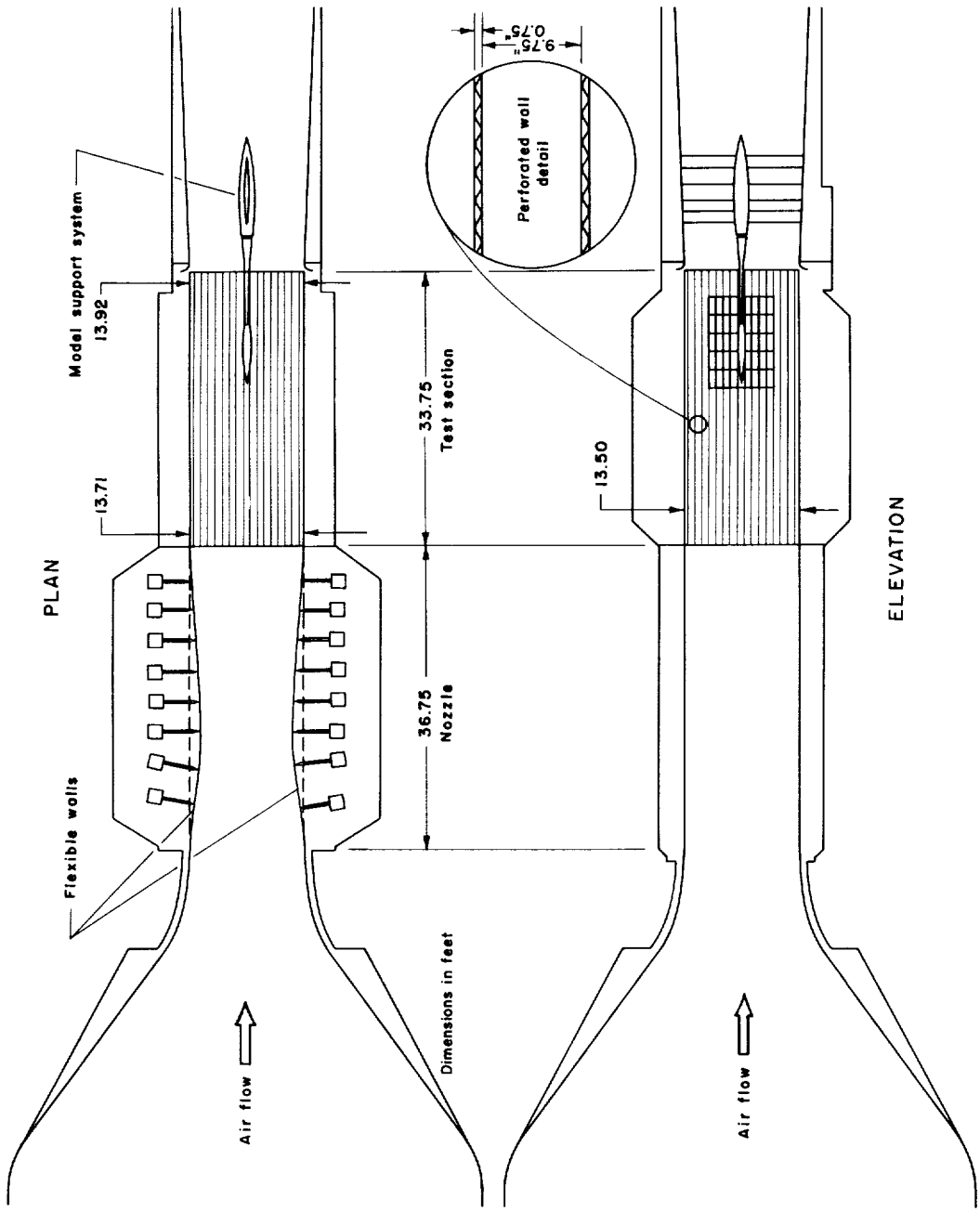

Figure 2.- General arrangement of the high-speed portion of the Ames 14-foot transonic wind tunnel.

Equation of forebodies: $r = r_o \left[1-\left(1-\frac{2x}{l}\right)^2\right]^{3/4}$

$r_o = 2$

$l = 50$

Equation of afterbody, $r = r_o$

$0 < x < 25$

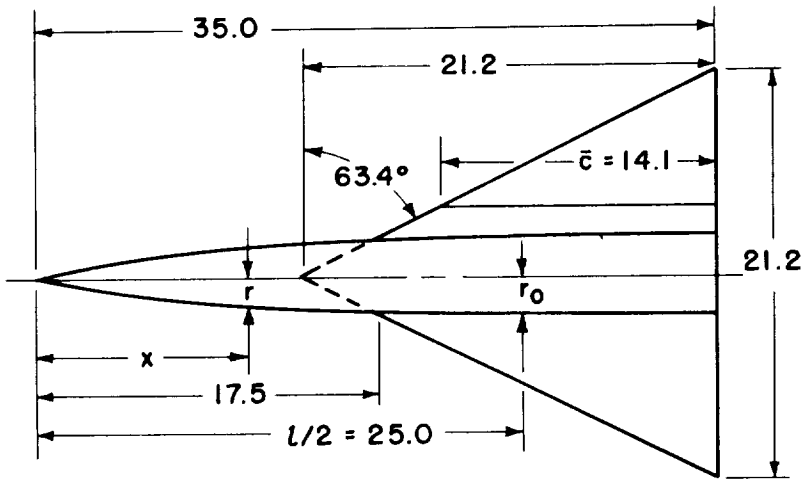

Dimensions in inches

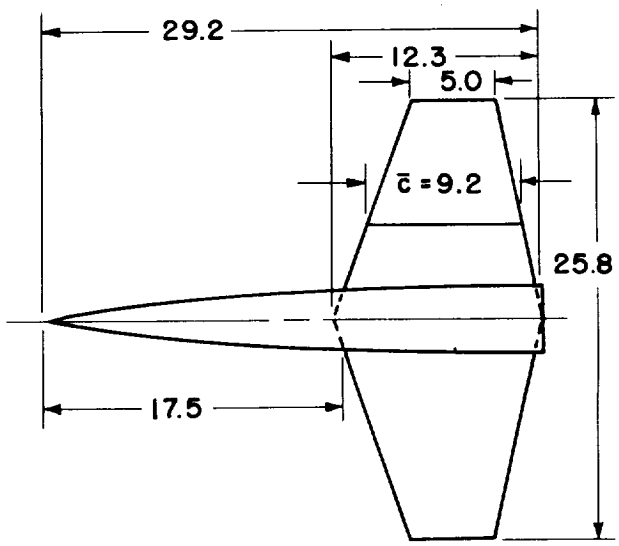

Figure 3.- Plan views of the wing-body combinations tested.

A-23678

Figure 4.- Photograph of the aspect-ratio-3, straight tapered wing-body combination mounted in the Ames 14-foot transonic wind tunnel.

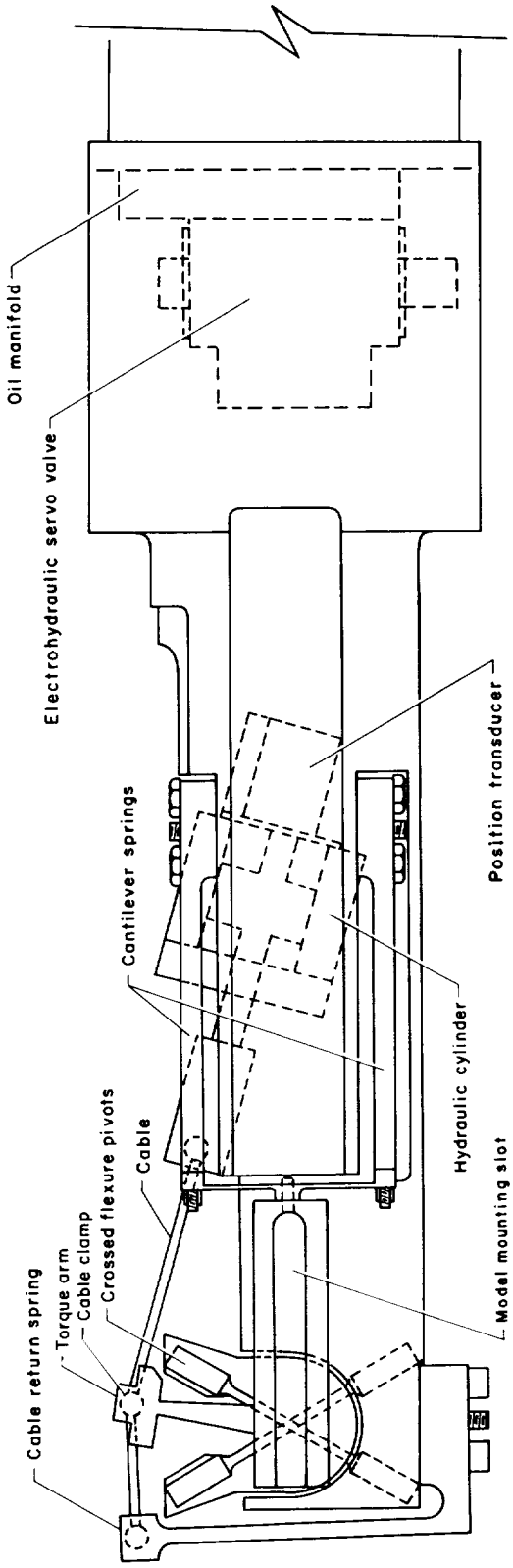

(a) Return spring and cable system.

Figure 5.- Assembled view of the dynamic balance and electrohydraulic drive.

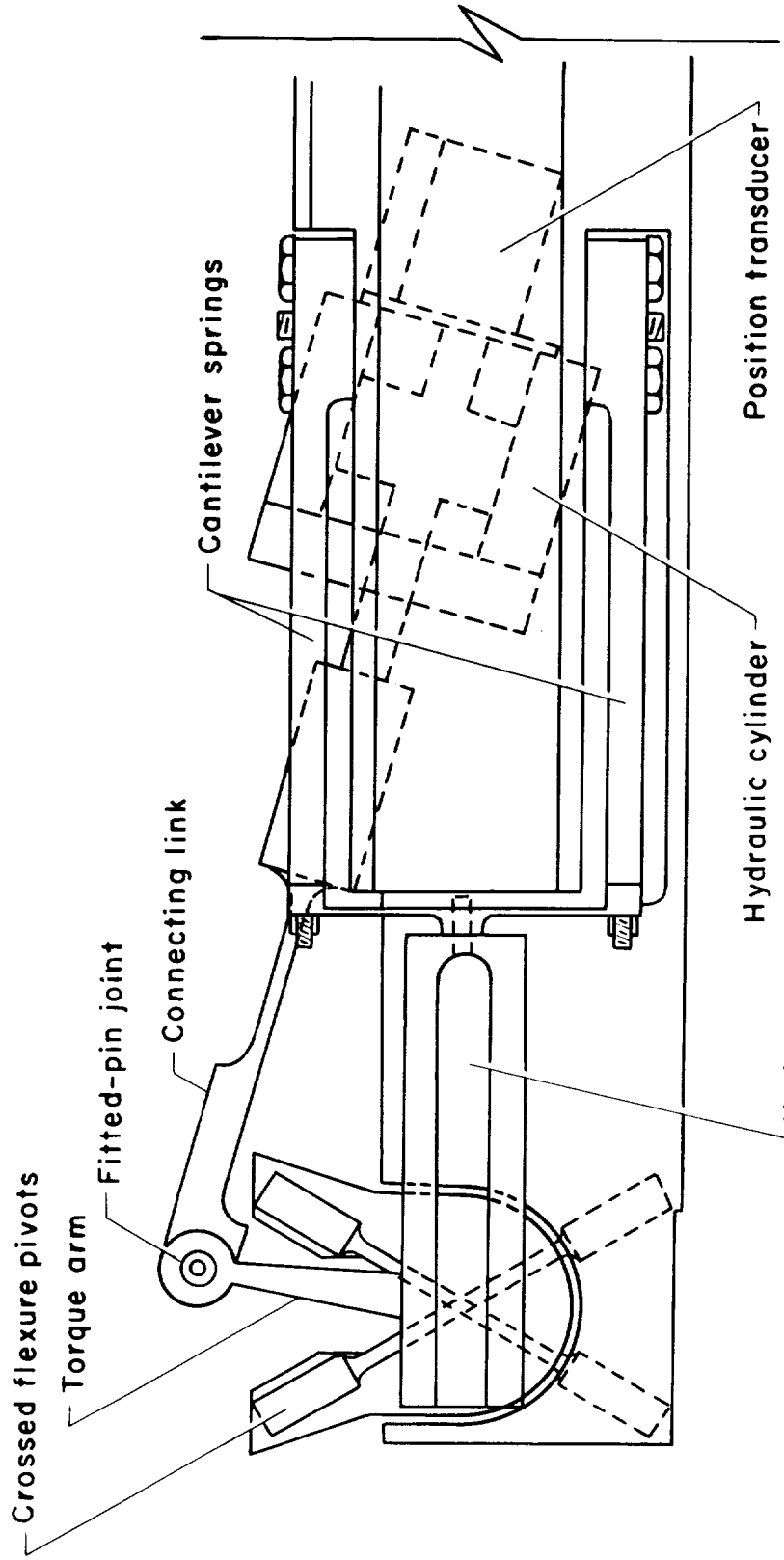

(b) Fitted pin and solid connecting link system.

Figure 5.- Concluded.

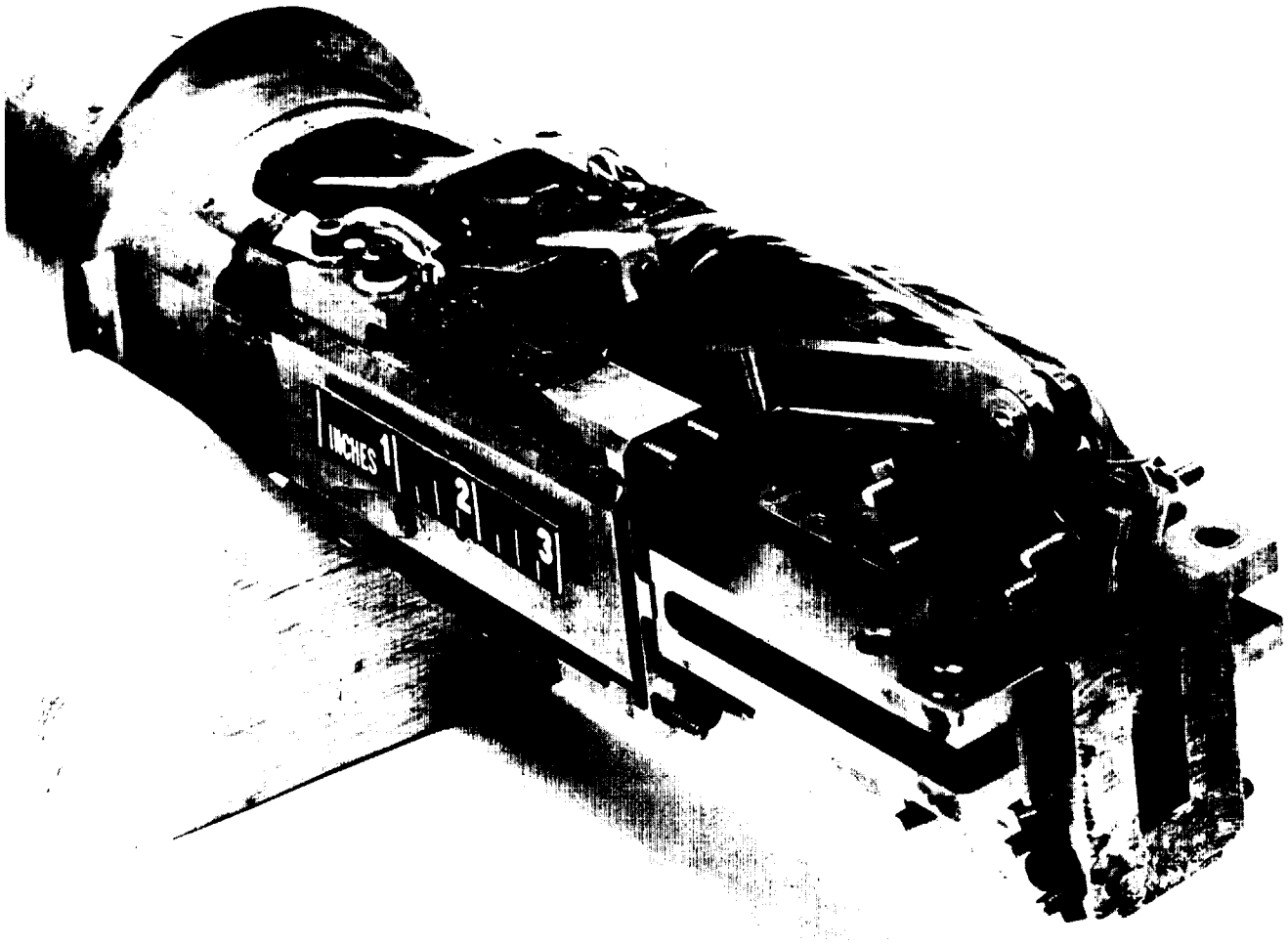

A-24032

Figure 6.- Photograph of the dynamic balance with solid connecting link drive.

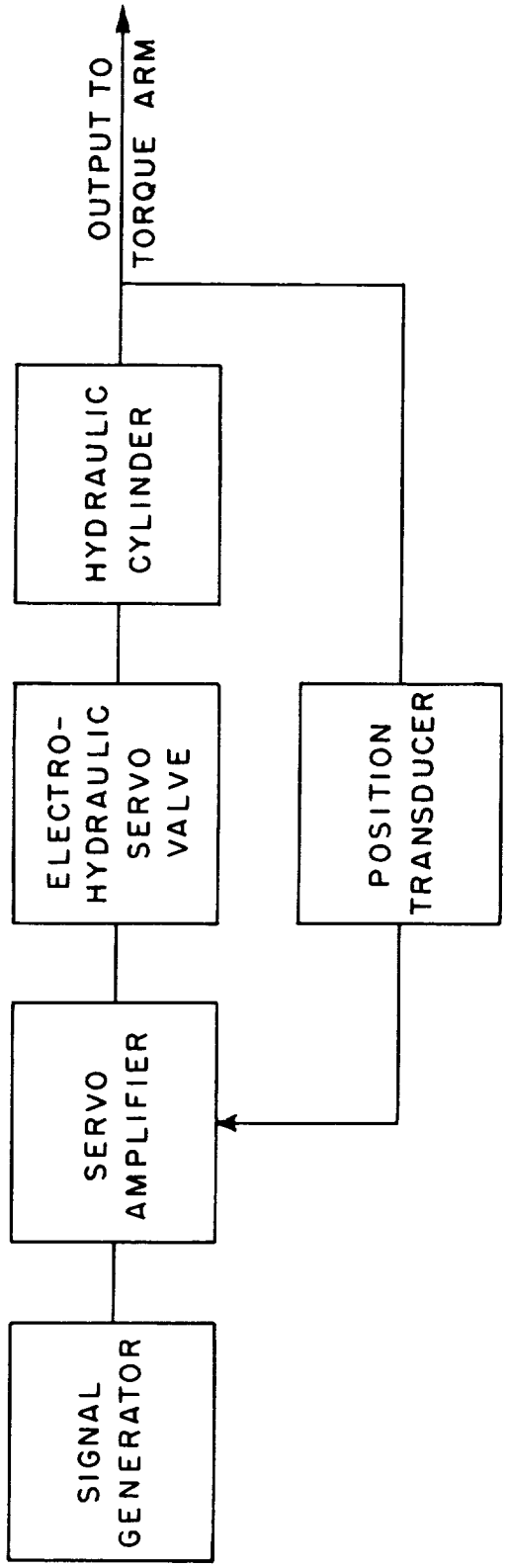

Figure 7.- Block diagram of electrohydraulic drive system.

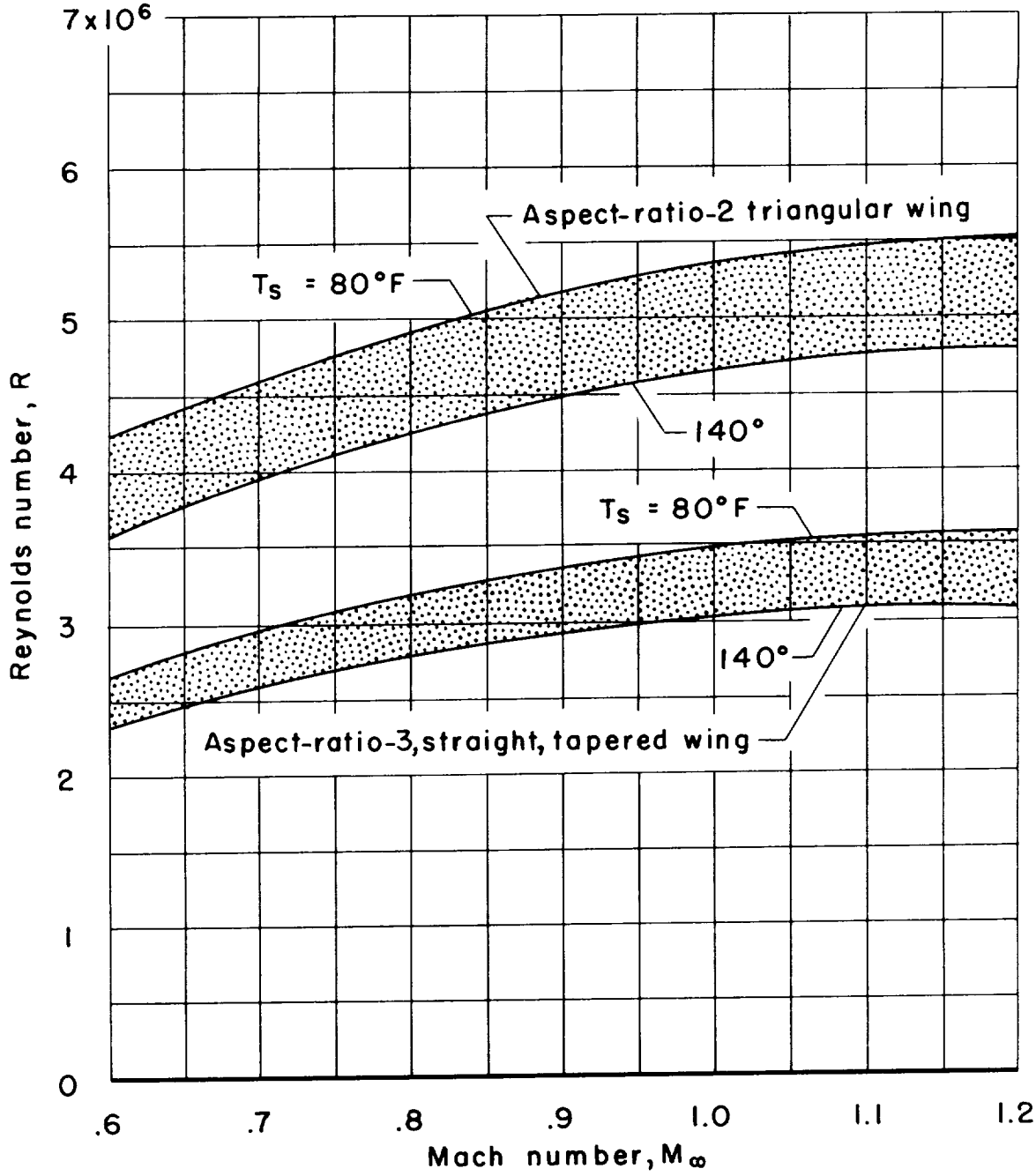

Figure 8.- Variation of Reynolds number with Mach number for the models investigated.

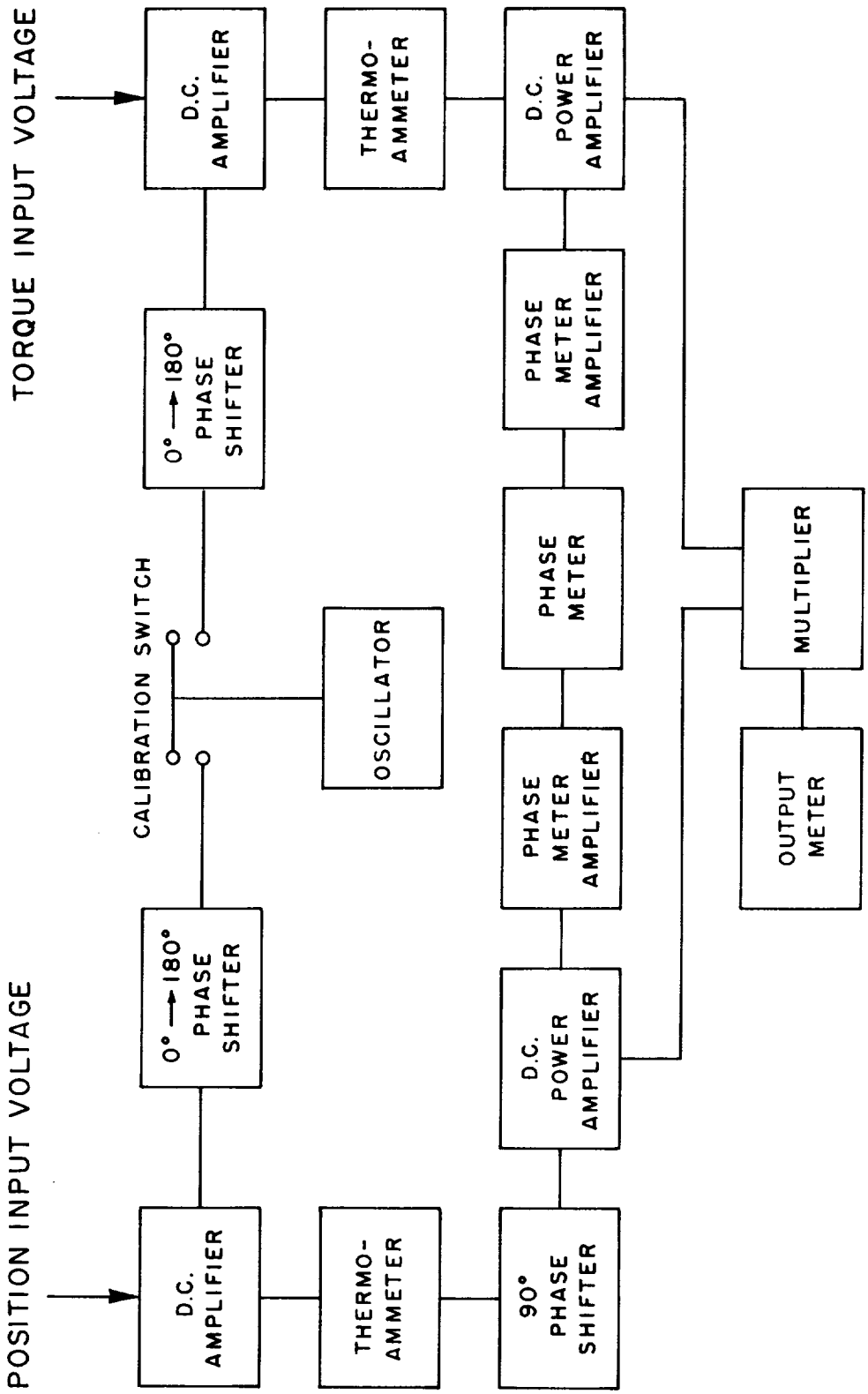

Figure 9.- Block diagram of the NACA Ames flutter analyzer.

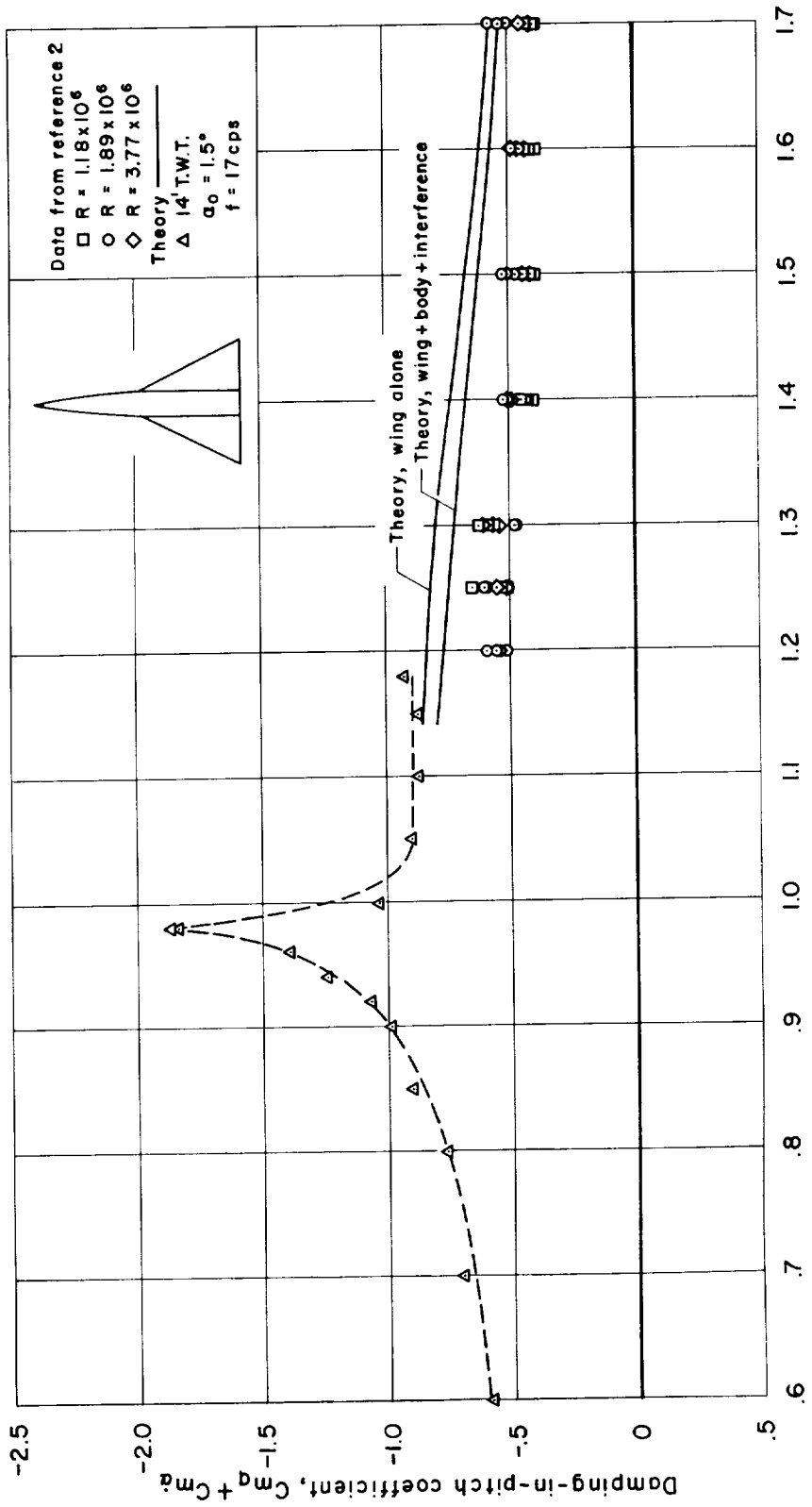

(a) Axis of rotation at 0.45 $\bar{c}$.

Figure 10.- Variation of damping-in-pitch coefficient with Mach number for the wing-body combination having a triangular wing of aspect ratio 2.

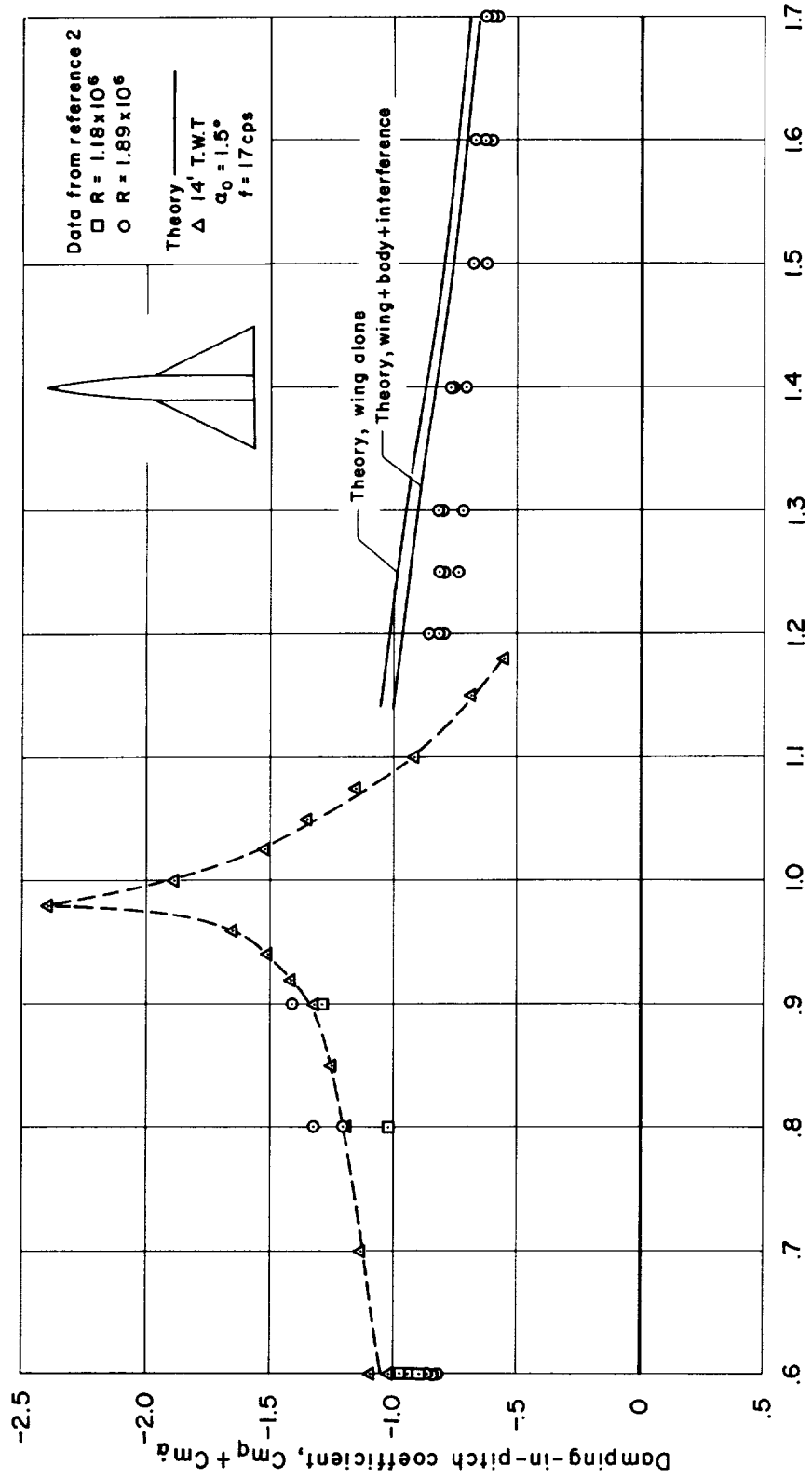

(b) Axis of rotation at 0.35 $\bar{c}$.

Figure 10.- Concluded.

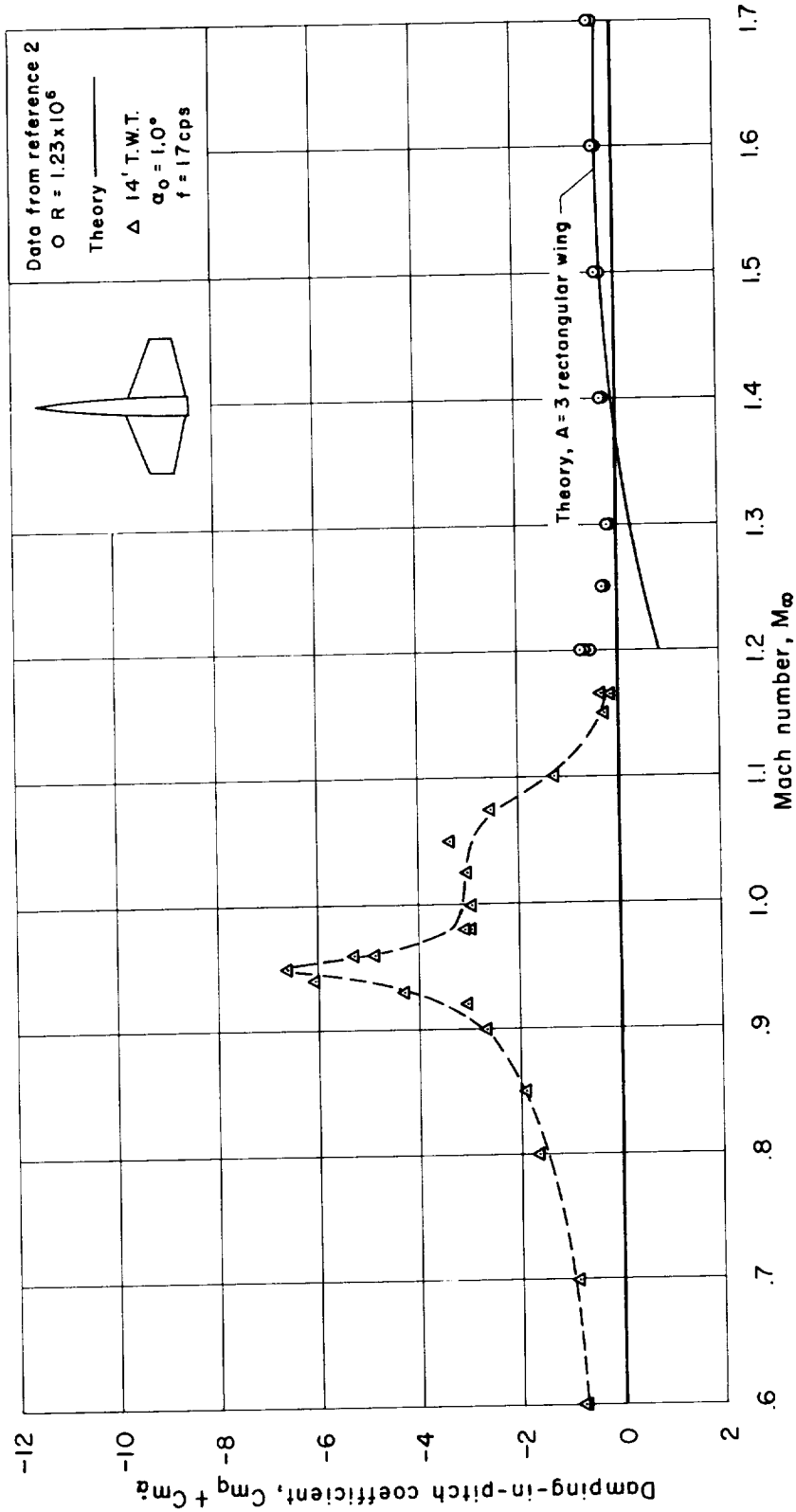

(a) Axis of rotation at 0.35 $\bar{c}$.

Figure 11.- Variation of damping-in-pitch coefficient with Mach number for the wing-body combination having an unswept wing of aspect ratio 3.

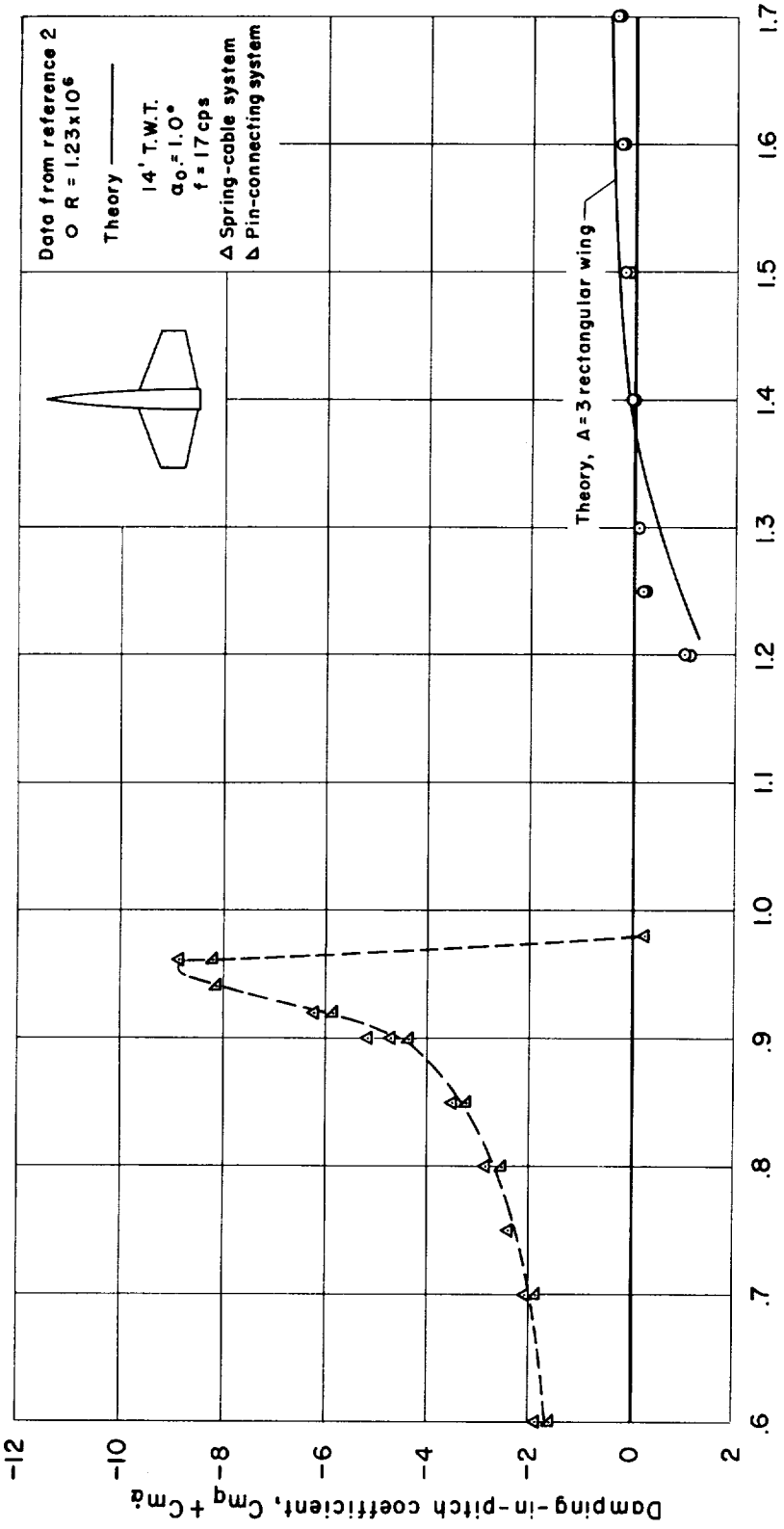

(b) Axis of rotation at 0.20 $\bar{c}$.

Figure 11.- Concluded.

NASA MEMO 11-30-58A
National Aeronautics and Space Administration.
EXPERIMENTAL WIND-TUNNEL INVESTIGATION OF THE TRANSONIC DAMPING-IN-PITCH CHARACTERISTICS OF TWO WING-BODY COMBINATIONS. Horace F. Emerson and Robert C. Robinson. December 1958. 26p. diagrs., photos. (NASA MEMORANDUM 11-30-58A)

The results of an experimental wind-tunnel investigation of the damping in pitch of two wing-body combinations are presented through the transonic Mach number range. One model had a straight, tapered wing of aspect ratio 3 and the second model had a triangular wing of aspect ratio 2. The Mach number range was from 0.60 to 1.18 and the Reynolds number varied from 2.3 million to 5.5 million. The results were obtained by a forced-oscillation technique in which an electrohydraulic servo valve was used to power the drive system.

Copies obtainable from NASA, Washington

1. Stability, Longitudinal - Dynamic (1.8.1.2.1)
2. Damping Derivatives - Stability (1.8.1.2.3)
3. Research Technique, Aerodynamics (9.2.2)

I. Emerson, Horace F.
II. Robinson, Robert C.
III. NASA MEMO 11-30-58A

NASA

NASA MEMO 11-30-58A
National Aeronautics and Space Administration.
EXPERIMENTAL WIND-TUNNEL INVESTIGATION OF THE TRANSONIC DAMPING-IN-PITCH CHARACTERISTICS OF TWO WING-BODY COMBINATIONS. Horace F. Emerson and Robert C. Robinson. December 1958. 26p. diagrs., photos. (NASA MEMORANDUM 11-30-58A)

The results of an experimental wind-tunnel investigation of the damping in pitch of two wing-body combinations are presented through the transonic Mach number range. One model had a straight, tapered wing of aspect ratio 3 and the second model had a triangular wing of aspect ratio 2. The Mach number range was from 0.60 to 1.18 and the Reynolds number varied from 2.3 million to 5.5 million. The results were obtained by a forced-oscillation technique in which an electrohydraulic servo valve was used to power the drive system.

Copies obtainable from NASA, Washington

1. Stability, Longitudinal - Dynamic (1.8.1.2.1)
2. Damping Derivatives - Stability (1.8.1.2.3)
3. Research Technique, Aerodynamics (9.2.2)

I. Emerson, Horace F.
II. Robinson, Robert C.
III. NASA MEMO 11-30-58A

NASA

NASA MEMO 11-30-58A
National Aeronautics and Space Administration.
EXPERIMENTAL WIND-TUNNEL INVESTIGATION OF THE TRANSONIC DAMPING-IN-PITCH CHARACTERISTICS OF TWO WING-BODY COMBINATIONS. Horace F. Emerson and Robert C. Robinson. December 1958. 26p. diagrs., photos. (NASA MEMORANDUM 11-30-58A)

The results of an experimental wind-tunnel investigation of the damping in pitch of two wing-body combinations are presented through the transonic Mach number range. One model had a straight, tapered wing of aspect ratio 3 and the second model had a triangular wing of aspect ratio 2. The Mach number range was from 0.60 to 1.18 and the Reynolds number varied from 2.3 million to 5.5 million. The results were obtained by a forced-oscillation technique in which an electrohydraulic servo valve was used to power the drive system.

Copies obtainable from NASA, Washington

1. Stability, Longitudinal - Dynamic (1.8.1.2.1)
2. Damping Derivatives - Stability (1.8.1.2.3)
3. Research Technique, Aerodynamics (9.2.2)

I. Emerson, Horace F.
II. Robinson, Robert C.
III. NASA MEMO 11-30-58A

NASA

NASA MEMO 11-30-58A
National Aeronautics and Space Administration.
EXPERIMENTAL WIND-TUNNEL INVESTIGATION OF THE TRANSONIC DAMPING-IN-PITCH CHARACTERISTICS OF TWO WING-BODY COMBINATIONS. Horace F. Emerson and Robert C. Robinson. December 1958. 26p. diagrs., photos. (NASA MEMORANDUM 11-30-58A)

The results of an experimental wind-tunnel investigation of the damping in pitch of two wing-body combinations are presented through the transonic Mach number range. One model had a straight, tapered wing of aspect ratio 3 and the second model had a triangular wing of aspect ratio 2. The Mach number range was from 0.60 to 1.18 and the Reynolds number varied from 2.3 million to 5.5 million. The results were obtained by a forced-oscillation technique in which an electrohydraulic servo valve was used to power the drive system.

Copies obtainable from NASA, Washington

1. Stability, Longitudinal - Dynamic (1.8.1.2.1)
2. Damping Derivatives - Stability (1.8.1.2.3)
3. Research Technique, Aerodynamics (9.2.2)

I. Emerson, Horace F.
II. Robinson, Robert C.
III. NASA MEMO 11-30-58A

NASA